

# Baryons, Dark Matter, and the Jeans Mass in Simulations of Cosmological Structure Formation

J. Michael Owen

Department of Astronomy, Ohio State University, Columbus, OH 43210 USA

Email: [owen@payne.mps.ohio-state.edu](mailto:owen@payne.mps.ohio-state.edu)

Jens V. Villumsen

Max Planck Institut für Astrophysik, Karl Schwarzschild Strasse 1, 85740 Garching bei Munchen, Germany

Email: [jens@mpa-garching.mpg.de](mailto:jens@mpa-garching.mpg.de)

## ABSTRACT

We investigate the properties of hybrid gravitational/hydrodynamical simulations, examining both the numerics and the general physical properties of gravitationally driven, hierarchical collapse in a mixed baryonic/dark matter fluid. We demonstrate that, under certain restrictions, such simulations converge with increasing resolution to a consistent solution. The dark matter achieves convergence provided that the relevant scales dominating nonlinear collapse are resolved. If the gas has a minimum temperature (as expected, for example, when intergalactic gas is heated by photoionization due to the ultraviolet background) *and* the corresponding Jeans mass is resolved, then the baryons also converge. However, if there is no minimum baryonic collapse mass or if this scale is not resolved, then the baryon results err in a systematic fashion. In such a case, as resolution is increased the baryon distribution tends toward a higher density, more tightly bound state. We attribute this to the fact that under hierarchical structure formation on all scales there is always an earlier generation of smaller scale collapses, causing shocks which irreversibly alter the state of the baryon gas. In a simulation with finite resolution we therefore always miss such earlier generation collapses, unless a physical scale is introduced below which such structure formation is suppressed in the baryons. We also find that the baryon/dark matter ratio follows a characteristic pattern, such that collapsed structures possess a baryon enriched core (enriched by factors  $\sim 2$  or more over the universal average) which is embedded within a dark matter halo, even without accounting for radiative cooling of the gas. The dark matter is unaffected by changing the baryon distribution (at least in the dark matter dominated case investigated here), allowing hydrodynamics to alter the distribution of visible material in the universe from that of the underlying mass.

*Subject headings:* Cosmology: theory — Hydrodynamics — Large scale structure of the universe — Methods: numerical

## 1. Introduction

Hydrodynamics is thought to play a key role in the formation of the visible structures in the universe, such as bright galaxies and hot intracluster gas. For this reason there is a great deal of interest in incorporating hydrodynamical effects into cosmological structure formation simulations in order to make direct, quantitative comparisons of such simulations to observed data. In addition to gravitation, a cosmological hydrodynamical simulation must minimally account for pressure support, shock physics, and radiative cooling, as these are the fundamental physical processes thought to play a dominant role in the formation of large, bright galaxies (White & Rees 1978). There is already a bewildering array of such studies published, including Cen & Ostriker (1992a,b), Katz, Hernquist, & Weinberg (1992), Evrard, Summers, & Davis (1994), Navarro & White (1994), and Steinmetz & Müller (1994), to name merely a few. In order to appreciate the implications of such ambitious studies, it is important that we fully understand both the physical effects of hydrodynamics under a cosmological framework and the numerical aspects of the tools used for such investigations. Basic questions such as how the baryon to dark matter ratio varies in differing structures (galaxies, clusters, and filaments) and exactly how this is affected by physical processes such as shock heating, pressure support, or radiative cooling remain unclear. It is also difficult to separate real physical effects from numerical artifacts, particularly given the current limitations on the resolution which can be achieved. For example, in a recent study of X-ray clusters Anninos & Norman (1996) find the observable characteristics of a simulated cluster to be quite resolution dependent, with the integrated X-ray luminosity varying as  $L_x \propto (\Delta x)^{-1.17}$ , core radius  $r_c \propto (\Delta x)^{0.6}$ , and emission weighted temperature  $T_X \propto (\Delta x)^{0.35}$  (where  $\Delta x$  is the gridcell size of the simulation). In a study of the effects of photoionization on galaxy formation, Weinberg, Hernquist, & Katz (1996) find that the complex interaction of numerical effects (such as resolution) with microphysical effects (such as radiative cooling and photoionization heating) strongly influences their resulting model galaxy population. In this paper we focus on separating physical from numerical effects in a series of idealized cosmological hydrodynamical simulations. This study is intended to be an exploratory survey of hydrodynamical cosmology, similar in spirit to the purely gravitational studies of Melott & Shandarin (1990), Beacom et al. (1991), and Little, Weinberg, & Park (1991).

We will examine the effects of pressure support and shock heating in a mixed baryonic/dark matter fluid undergoing gravitationally driven hierarchical collapse. This problem is approached with two broad questions in mind: how stable and reliable is the numerical representation of the system, and what can we learn about the physics of such collapses? These questions have been investigated for purely gravitational systems in studies such as those mentioned above. In those studies numerically it is found that the distribution of collisionless matter converges to consistent states so long as the nonlinear collapse scale is resolved. Such convergence has not been demonstrated for collisional systems, however. It is not clear that hydrodynamical simulations will demonstrate such convergence in general, nor if they do that the nonlinear scale is the crucial scale which must be resolved. Hydrodynamical processes are dominated by localized interactions on small scales, allowing the smallest scales to substantially affect the state of the baryonic gas. As an example, consider a collisional fluid undergoing collapse. Presumably such a system will undergo shocking near the point of maximal collapse, allowing a large fraction of the kinetic energy of the gas to be converted to thermal energy. In a simple case such as a single plane-wave perturbation (the Zel'dovich pancake collapse), the obvious scale which must be resolved is the scale of the shock which forms around the caustic. However, in a hierarchical structure formation scenario there is a hierarchy of collapse scales, and for any given resolution limit there is always a smaller scale which will undergo nonlinear collapse. The subsequent evolution of the gas could well depend upon how well such small scale interactions are resolved, and changes in the density and temperature of gas on small scales could in turn influence how it behaves on larger scales (especially if cooling is important).

In this paper we examine a series of idealized experiments, evolving a mixed fluid of baryons and collisionless dark matter (dark matter dominated by mass), coupled gravitationally in a flat, Einstein-de Sitter cosmology. The mass is seeded with Gaussian distributed initial density perturbations with a power-law initial power spectrum. We perform a number of simulations, varying the resolution, the initial cutoff in the density perturbation spectrum, and the minimum allowed temperature for the baryons. Enforcing a minimum temperature for the baryons implies there will be a minimal level of pressure support, and therefore a minimum collapse scale (the Jeans mass), below which the baryons are pressure supported against collapse. From the numerical point of view, performing a number of simulations with identical initial physical conditions but varying resolution allows us to unambiguously identify resolution effects. By enforcing a Jeans mass for the baryons we introduce an intrinsic mass scale to the problem, which may or may not be resolved in any individual experiment. The hope is that even if the gas dynamical results do not converge with increasing resolution in the most general case, the system will converge if the fundamental Jeans mass is resolved.

The effects of the presence (or absence) of a baryonic Jeans mass also raises interesting physical questions. Though we simply impose arbitrary minima for the baryon temperatures here, processes such as photoionization enforce minimum temperatures in the real universe by injecting thermal energy into intergalactic gas. The Gunn-Peterson test indicates that the intergalactic medium is highly ionized (and therefore at temperatures  $T \gtrsim 10^4$ K) out to at least  $z \lesssim 5$ . Shapiro, Giroux, & Babul (1994) discuss these issues for the intergalactic medium. The dark matter, however, is not directly influenced by this minimal pressure support in the baryons, and therefore is capable of collapsing on arbitrarily small scales. Pressure support provides a mechanism to separate the two species, and since the dark matter dominates the mass density it can create substantial gravitational perturbations on scales below the Jeans mass. While there are many studies of specific cosmological models with detailed microphysical assumptions, the general problem of the evolution of pressure supported baryons in the presence of nonlinear dark matter starting from Gaussian initial conditions has not been investigated in a systematic fashion.

This paper is organized as follows. In §2 we discuss the particulars of how the simulations are constructed and performed. In §3 we characterize the numerical effects we find in these simulations, and in §4 we discuss our findings about the physics of this problem. Finally, §5 summarizes the major results of this investigation.

## 2. The Simulations

A survey such as this optimally requires a variety of simulations in order to adequately explore the range of possible resolutions and input physics. Unfortunately, hydrodynamical cosmological simulations are generally quite computationally expensive, and therefore in order to run a sufficiently broad number of experiments we restrict this study to 2-D simulations. There are two primary advantages to working in 2-D rather than 3-D. First, parameter space can be more thoroughly explored, since the computational cost per simulation is greatly reduced and a larger number of simulations can be performed. Second, working in 2-D enables us to perform much higher resolution simulations than are feasible in 3-D. While the real universe is 3-D and we must therefore be cautious about making specific quantitative predictions based on this work, 2-D experiments can be used to yield valuable qualitative insights into the behaviour of these systems. For similar reasons Melott & Shandarin (1990) and Beacom et al. (1991) also utilize 2-D simulations in their studies of purely gravitational dynamics.

The 2-D simulations presented here can be interpreted as a slice through an infinite 3-D simulation (periodic in  $(x, y)$  and infinite in  $z$ ). The particles interact as parallel rods

of infinite length, obeying a gravitational force law of the form  $F_{\text{grav}} \propto 1/r$ . The numerical technique used for all simulations is SPH (Smoothed Particle Hydrodynamics) for the hydrodynamics and PM (Particle-Mesh) for the gravitation. The code and technique are described and tested in Owen et al. (1996), so we will not go into much detail here. We do note, however, that while our code implements ASPH (Adaptive Smoothed Particle Hydrodynamics) as described in our initial methods paper, we are not using the tensor smoothing kernel of ASPH for this investigation, but rather simple SPH. The results should be insensitive to such subtle technique choices since the goal is to compare simulation to simulation, so we employ simple SPH in order to separate our findings from questions of technique.

All simulations are performed under a flat, Einstein-de Sitter cosmology, with 10% baryons by mass ( $\Omega_{\text{bary}} = 0.1, \Omega_{\text{dm}} = 0.9, \Lambda = 0$ ). Thus the mass density is dominated by the collisionless dark matter, which is linked gravitationally to the collisional baryons. The baryon and dark matter particles are initialized on the same perturbed grid, with equal numbers of both species. Therefore, initially all baryons exactly overlie the dark matter particles, and only hydrodynamical effects can separate the two species. The baryon/dark matter mass ratio is set by varying the particle mass associated with each species. The initial density perturbation spectrum is taken to be a power-law  $P(k) = \langle |\delta\rho(k)/\bar{\rho}|^2 \rangle \propto k^n$  up to a cutoff frequency  $k_c$ . Note that since these are 2-D simulations, for integrals over the power spectrum this is equivalent in the 3-D to a power spectrum of index  $n - 1$ . In this paper we adopt a “flat” ( $n = 0$ ) 2-D spectrum

$$P_{\text{2-D}}(k) = A_{\text{norm}} \begin{cases} k^0 & : k \leq k_c \Rightarrow P_{\text{3-D}}(k) = k^{-1} \\ 0 & : k > k_c, \end{cases} \quad (1)$$

where  $A_{\text{norm}}$  normalizes the power-spectrum. Note that using a flat cosmology and power-law initial conditions implies these simulations are scale-free, and should evolve self-similarly in time. We can choose to assign specific scales to the simulations in order to convert the scale-free quantities to physical units. All simulations are halted after 60 expansion factors, at which point the nonlinear scale (the scale on which  $\delta\rho/\rho \sim 1$ ) is roughly 1/8 of the box size.

The Jeans length is the scale at which pressure support makes the gas stable against the growth of linear fluctuations due to self-gravitation – the Jeans mass is the amount of mass contained within a sphere of diameter the Jeans length. The Jeans length  $\lambda_J$  and mass  $M_J$  are defined by the well known formula (Binney & Tremaine 1987)

$$\lambda_J = \left( \frac{\pi c_s^2}{G\rho} \right)^{1/2}, \quad (2)$$

$$M_J = \frac{4\pi}{3}\rho \left(\frac{1}{2}\lambda_J\right)^3 = \frac{\pi\rho}{6} \left(\frac{\pi c_s^2}{G\rho}\right)^{3/2}, \quad (3)$$

where  $\rho$  is the mass density and  $c_s$  the sound speed. The baryons are treated as an ideal gas obeying an equation of state of the form  $P = (\gamma - 1)u\rho$ , where  $P$  is the pressure and  $u$  is the specific thermal energy. Enforcing a minimum specific thermal energy (and therefore temperature) in the gas forces a minimum in the sound speed  $c_s^2 = \gamma P/\rho = \gamma(\gamma - 1)u$ , which therefore implies we have a minimum Jeans mass through equation (3). Note that  $\rho$  is the total mass density (baryons and dark matter), since it is the total gravitating mass which counts, and therefore  $M_J$  as expressed in equation (3) represents the total mass contained within  $r \leq \lambda_J/2$ . If we want the total baryon mass contained within this radius, we must multiply  $M_J$  by  $\Omega_{\text{bary}}/\Omega$ .

It is also important to understand how the mass resolution is set for the baryons by the SPH technique. This is not simply given by the baryon particle mass, since SPH interpolation is a smoothing process typically extending over spatial scales of several interparticle spacings. In general the mass resolution for the hydrodynamic calculations can be estimated as the amount of mass enclosed by a typical SPH interpolation volume. If the SPH smoothing scale is given by  $h$  and the SPH sampling extends for  $\eta$  smoothing scales, then the mass resolution  $M_R$  is given by

$$M_R = \frac{4}{3}\pi(\eta h)^3\rho. \quad (4)$$

This is probably something of an overestimate, since the weight for each radial shell in this interpolation volume (given by the SPH sampling kernel  $W$ ) falls off smoothly towards  $r = \eta h$ , but given the other uncertainties in this quantity equation (4) seems a reasonable estimate. Note that the resolution limit for the SPH formalism is best expressed in terms of a mass limit, appropriate for SPH's Lagrangian nature. For this reason we choose to express the Jeans limit in terms of the Jeans mass (eq. [3]) throughout this work, as the Jeans limit can be equally expressed in terms of a spatial or a mass scale. In N-body work it is common to express the mass resolution of an experiment in units of numbers of particles. In our simulations we use a bi-cubic spline kernel which extends to  $\eta = 2$  smoothing lengths, and initialize the smoothing scales such that the smoothing scale  $h$  extends for two particle spacings. We therefore have a mass resolution in 2-D of roughly 50 particles, or equivalently in 3-D roughly 260 particles.

We perform simulations both with and without a minimum temperature (giving Jeans masses  $M_J = 0$ ,  $M_J > 0$ ), at three different resolutions ( $N = N_{\text{bary}} = N_{\text{dm}} = 64^2$ ,  $128^2$ , and  $256^2$ ), and for three different cutoffs in the initial perturbation spectrum ( $k_c = 32$ ,  $64$ , and  $128$ ). The initial density perturbations are initialized as Gaussian distributed with

random phases and amplitudes, but in such a manner that all simulations have identical phases and amplitudes up to the imposed cutoff frequency  $k_c$ . The cutoff frequencies are the subset of  $k_c \in (32, 64, 128)$  up to the Nyquist frequency for each resolution  $k_{\text{Nyq}} = N^{1/2}/2$ , so for each resolution we have  $k_c(N = 64^2) = 32$ ,  $k_c(N = 128^2) \in (32, 64)$ , and  $k_c(N = 256^2) \in (32, 64, 128)$ . For each value of the minimum temperature we therefore have a grid of simulations which either have the same input physics at differing resolutions (*i.e.*,  $k_c = 32$  for  $N \in [64^2, 128^2, 256^2]$ ), or varying input physics at fixed resolution (*i.e.*,  $N = 256^2$  for  $k_c \in [32, 64, 128]$ ). This allows us to isolate and study both numerical and physical effects during the evolution of these simulations. In total we discuss twelve simulations.

For the simulations with a minimum temperature, there is an ambiguity in assigning a global Jeans mass with that temperature. The density in equation (3) is formally the *local* mass density, and therefore the Jeans mass is in fact position dependent through  $\rho(\vec{r})$ . Throughout this work we will refer to the Jeans mass at any given expansion factor as the Jeans mass defined using a fixed minimum temperature and the average background density, making this mass scale a function of time only. This is equivalent to taking the zeroth order estimate of  $M_J$ , giving us a well defined characteristic mass scale. In terms of this background density, Figure 1 shows the baryon Jeans mass (in units of the resolved mass via equation [4]) as a function of expansion. Note that for a given simulation  $M_R$  remains fixed, and it is the Jeans mass which grows as  $M_J \propto \rho^{-1/2} \propto a^{3/2}$ . It is apparent that the  $N = 256^2$  simulations resolve the Jeans mass throughout most of the evolution, the  $N = 128^2$  simulations resolve  $M_J$  by  $a/a_i \sim 15$ , and the  $N = 64^2$  simulation does not approach  $M_J/M_R \sim 1$  until the end of our simulations at  $a/a_i \sim 60$ . The specific value of  $T_{\min}$  used in this investigation is chosen to yield this behaviour. We discuss physically motivated values for this minimum temperature in §5.

### 3. Numerical Resolution and the Jeans Mass

#### 3.1. Dark Matter

We will begin by examining the dark matter distribution, as this is a problem which has been examined previously. Figures 2a and b show images of the dark matter overdensity  $\rho_{\text{dm}}/\bar{\rho}_{\text{dm}}$  for the  $M_J = 0$  simulations. In order to fairly compare with equivalent images of the SPH baryon densities, the dark matter information is generated by assigning a pseudo-SPH smoothing scale to each dark matter particle, such that it samples roughly the same number of neighboring dark matter particles as the SPH smoothing scale samples in the baryons. We then use the normal SPH summation method to assign dark matter

densities, which are used to generate these images. The panels in the figure are arranged with increasing simulation resolution  $N$  along rows, and increasing cutoff frequency  $k_c$  down columns. The diagonal panels represent each resolution initialized at its Nyquist frequency for  $P(k)$ . Note that the physics of the problem is constant along rows, and numerics is constant along columns. If resolution were unimportant, the results along rows should be identical. Likewise, since the numerics is held constant along columns, only physical effects can alter the results in this direction.

Comparing the dark matter densities along the rows of Figure 2a, it is clear that the structure becomes progressively more clearly defined as the resolution increases. This is to be expected, since the higher resolution simulations can resolve progressively more collapsed/higher density structures. The question is whether or not the underlying particle distribution is systematically changing with resolution. In other words, do the simulations converge to the same particle distribution on the scales which are resolved? Figure 2b shows this same set of dark matter overdensities for the  $M_J = 0$  simulations, only this time each simulation is degraded to an equivalent  $N = 64^2$  resolution and resampled. This is accomplished by selecting every  $n$ th node from the higher resolution simulations, throwing away the rest and suitably modifying the masses and smoothing scales of the selected particles. Note that now the dark matter distributions look indistinguishable for the different resolution experiments, at least qualitatively. This similarity implies that the high frequency small scale structure has minimal effect on the larger scales resolved in this figure. Looking down the columns of Figure 2a it is clear that increasing  $k_c$  does in fact alter the dark matter particle distribution, such that the large scale, smooth filaments are progressively broken up into smaller clumps aligned with the overall filamentary structure. These differences are lost in the low-res results of Figure 2b, implying that these subtle changes do not significantly affect the large scale distribution of the dark matter.

In Figures 3a and b we show the mass distribution functions for the dark matter overdensity  $f(\rho_{\text{dm}}/\bar{\rho}_{\text{dm}})$ . Figure 3a includes all particles from each simulation (as in Figure 2a), while Figure 3b is calculated for each simulation degraded to equivalent  $N = 64^2$  resolutions (comparable to Figure 2b). The panels are arranged as in Figure 2, with  $M_J = 0$  and  $M_J > 0$  overplotted as different line types. It is clear that the varying Jeans mass in the baryons has negligible effect on the dark matter, a point we will return to in §4. The full resolution results of Figure 3a show a clear trend for a larger fraction of the mass to lie at higher densities with increasing resolution. There is also a similar though weaker trend with increasing  $k_c$ . However, examining the resampled results of Figure 3b it appears that the results of all simulations converge, bearing out the visual impressions of Figures 2a and b. For the dark matter, with increasing resolution more information is gained about the highest density/most collapsed fraction of the mass, but so long as the pertinent

nonlinear scales are resolved the results converge. The underlying particle distribution does not depend upon the numerical resolution, similarly to the results discussed in Little et al. (1991).

### 3.2. Baryons

We now turn our attention to the baryon distribution. Figures 4a, b, c, and d show images of the baryon overdensity for  $M_J = 0$  and  $M_J > 0$  at expansions  $a/a_i = 30$  and  $a/a_i = 60$ . There is a pronounced trend for the collapsed filaments and clumps to become progressively more strongly defined as the simulation resolution improves – even more so than we see in the dark matter. The tendency to break up filaments into small scale clumps with increasing  $k_c$  is also clearly evident for the  $M_J = 0$  case. Additionally, the presence of a nonzero Jeans mass visibly influences the baryon density distribution in Figures 4c and d. This is particularly evident in the high resolution  $N = 256^2$  column, where the increased pressure support creates a “puffier” distribution, wiping out the smallest scale structures in the baryons. Recall from Figure 1 that we naively expect the presence of the pressure support for  $M_J > 0$  to affect both  $N = 128^2$  and  $N = 256^2$  at  $a/a_i = 30$ , but not  $N = 64^2$ . Comparing the results of Figures 4a and c, we indeed see this trend. By  $a/a_i = 60$ , the effects of the Jeans mass are clearly evident (comparing Figures 4b and d) for  $N = 128^2$  and  $N = 256^2$ , though  $N = 64^2$  still appears relatively unaffected.

Figures 5a and b show images of the baryon densities for the  $k_c = 32$  simulations, but in this case resampled to  $N = 64^2$  resolutions analogous to Figure 2b. At expansion  $a/a_i = 30$  (Figure 5a), we see that for  $M_J = 0$  the baryons appear to be systematically more tightly collapsed with increasing simulation resolution, even though they have all been resampled to the same sampling resolution to produce this image. This supports the view that the baryon distribution is fundamentally changing with increasing simulation resolution, in contrast with the dark matter. The  $N = 128^2$  and  $N = 256^2$   $M_J > 0$  simulations, however, demonstrate very similar baryon density images, though  $N = 64^2$  still appears different at  $a/a_i = 30$ . At  $a/a_i = 60$  (Figure 5b) we again see for  $M_J = 0$  a clear trend with simulation resolution, while the  $M_J > 0$  runs look remarkably similar to one another.

Figures 6a and b show the full resolution mass distribution functions of the baryon overdensities  $f(\rho_{\text{bary}}/\bar{\rho}_{\text{bary}})$  for all simulations at  $a/a_i = 30$  and  $a/a_i = 60$ , respectively. The  $M_J = 0$  functions show a strong trend to transfer mass from low to high densities with increasing resolution, and a similar though weaker trend with  $k_c$ . However, even at full resolution the  $M_J > 0$  simulations show very similar density distributions once  $M_J$  is resolved. The  $M_J > 0$  simulations also appear to be relatively insensitive to  $k_c$ , suggesting

that the increased small scale power is being wiped out by the pressure support. Figures 6c and d show these same baryon density distribution functions, only for all simulations degraded to  $N = 64^2$  resolutions. These bear out our previous observations. In the case with no Jeans mass, there is no sign of convergence in the baryon distribution as the resolution is increased. However, when a Jeans mass is present, then the baryon distributions do converge *once the Jeans mass is resolved*.

Figure 7 presents a more quantitative way to measure this convergence problem. In this figure we calculate the Kolmogorov-Smirnov statistic  $D(\rho_{\text{bary}})$ , comparing the baryon density distribution for each simulation to the others at the same expansion and Jeans mass. We do not expect these simulations to exactly reproduce one another, and therefore there is little point in assigning significance to the exact quantitative value of  $D$ . However, the K-S statistic does provide objective measures of how similar or dissimilar these distributions are, and therefore we might expect to learn something by comparing their relative values. Comparing the upper panels of Figure 7 we can see that at  $a/a_i = 30$  the  $N = 128^2$  and  $N = 256^2$  simulations are more similar for  $M_J > 0$  than for  $M_J = 0$ , while the  $N = 64^2$  simulation remains relatively distinct in both cases. At  $a/a_i = 60$ , however, we can see that for  $M_J > 0$  all the simulations appear comparable, while for  $M_J = 0$  they remain distinct for the different resolutions.

We therefore have a subtly different picture for the numerical behaviour of the dark matter and baryons. The critical resolution scale for the dark matter is the scale of nonlinearity. So long as this scale is resolved, the dark matter distribution can be expected to converge to a consistent state on resolved scales. Unfortunately, the distribution and state of the baryonic particles appears in general to be sensitive to the numerical resolution. However, it is possible and physically plausible to define a fundamental collapse scale in the form of the Jeans mass for the baryons, below which baryonic structure formation is suppressed. This scale can now be treated as the critical baryonic resolution scale, and we do find that once this threshold is reached the baryon distribution will reliably converge as well.

## 4. Hydrodynamics and the Baryon Distribution

### 4.1. Shocks and Temperatures

The results of the previous section indicate that hydrodynamical interactions on small scales can significantly alter the the final state of the baryons in ways which propagate upward and affect larger scales. The tendency for a simulation with a given finite resolution

is to underestimate the “true” fraction of high density, collapsed baryons. A likely cause for this trend is the presence of small scale, unresolved shocks in the baryon gas. Because shocks provide a mechanism for transferring the gas’s kinetic energy to thermal energy, it is reasonable to expect that the fashion and degree to which the baryons collapse will be dependent upon when and how strongly they undergo shocks. In this section we investigate the thermal state of the baryons, with the goal of understanding the pattern and importance of shocking in the gas.

In the top row of Figure 8 we show the 2-D mass distribution function of the baryons in terms of their overdensity and temperature  $f(\rho_{\text{bary}}/\bar{\rho}_{\text{bary}}, T)$  for the  $M_J = 0$  simulations at  $a/a_i = 60$ . The various resolutions share some gross properties in the  $\rho - T$  plane. The low density gas tends for the most part to be cool, though there is a tail of low density material with temperatures up to  $T \lesssim 10^4$ K. The high density gas is at relatively high temperatures, with most of the material near  $T \sim 10^6$ K. However, there is a notable trend for the highest density material to be somewhat cooler with increasing simulation resolution. This effect is similar to the behaviour seen in simple 1-D collapse such as the Zel’dovich pancake (Shapiro & Struck-Marcell 1985). The highest density gas is the fraction which collapses earliest, when the background density is highest. Such gas is placed on a lower adiabat than gas which falls in at later times, and thus remains cooler. In our case this means that since higher resolution simulations can resolve higher density clumps (which therefore form at earlier times), we should tend to see the temperature of the highest density material fall with increasing resolution.

The high temperature gas is heated by shocks as it falls into the dark matter dominated potential wells. In order to isolate shock heating from simple adiabatic compression heating, we calculate the distribution of the temperature in units of the adiabatic temperature  $T_{\text{ad}}$ , given by

$$T_{\text{ad}} = T_0 \left( \frac{\rho_{\text{bary}}}{\rho_0} \right)^{\gamma-1}. \quad (5)$$

$T_{\text{ad}}$  represents the temperature the gas would be at if it were only heated through simple  $PdV$  work. Since the only non-adiabatic process we allow is shock heating, only gas which has undergone shocking should be at  $T/T_{\text{ad}} > 1$ . In the bottom row of Figure 8 we calculate the distribution  $f(\rho_{\text{bary}}/\bar{\rho}_{\text{bary}}, T/T_{\text{ad}})$  for the  $M_J = 0$  simulations at  $a/a_i = 60$ . The high density fraction of the gas is clearly strongly shocked in all cases, with  $T/T_{\text{ad}} \sim 10^7 - 10^9$ . There is a clear trend for  $T/T_{\text{ad}}$  in the high density gas to fall with resolution, indicating that the highest density fraction of the gas is less strongly shocked as the resolution increases. Though we do not show the results at fixed resolution and increasing  $k_c$  here, there are also subtle trends evident with  $k_c$  in both the  $\rho - T$  and  $\rho - T/T_{\text{ad}}$  planes. Generally the temperature/shocking distribution of moderately overdense material grows

wider with increasing  $k_c$ .

It appears that shocks are indeed the key physical mechanism distinguishing the different resolution experiments. We find that in general most of the baryonic material is processed through shocks at some point. We note a general pattern in which the highest density gas in low resolution experiments is characteristically more strongly shocked than the highest density gas in higher resolution experiments. The physical inference of these trends is that the larger the region which collapses, the stronger the resulting shock. The underlying physical mechanism for this property is easily understood. Since the highest density material represents the gas which collapses earliest, this is also the gas which falls into the shallowest potential wells. As the structure continues to grow, these potential wells deepen. Gas which infalls at later times therefore picks up more kinetic energy, which in turn leads to stronger shocking and higher temperatures. Once shocking occurs, the state of the baryon gas is discontinuously and irreversibly altered. In order to properly represent the physical state of the gas, a simulation must resolve the smallest scales on which shocks are occurring. This is why enforcing a Jeans mass allows convergence, since establishing a minimum Jeans mass implies there is a minimum scale on which baryonic structures can form, forcing a minimum scale for shocking.

## 4.2. Comparing the Baryon & Dark Matter Distributions

One of the most fundamental questions we can address is how the distributions of dark matter and baryons compare to one another. Comparing the dark matter and baryon density fields for the  $M_J = 0$  case in Figures 2a and 4b, there is a distinct impression that the baryons tend to be more tightly clustered than the dark matter on all collapsed scales. The situation is a bit more complex for the  $M_J > 0$  case in Figure 4d. Comparing the ( $N = 256^2$ ,  $k_c = 128$ ) distributions, it is evident that the  $M_J > 0$  baryons show a more diffuse structure than that of the  $M_J = 0$  case, to the point that some of the smallest scale structures are entirely suppressed. Bear in mind that the dark matter evolves essentially independently of the baryons in this dark matter dominated case, so the small scale structures still form in the overall mass distribution – the baryons are simply excluded from them. The large scale structures such as the filaments and the largest knots are still quite prominent in the  $M_J > 0$  baryon distribution, just as for the  $M_J = 0$  case. These patterns suggest that the baryons are generically more clustered than the dark matter, down to the scale set by the Jeans mass. At this scale and lower, the dark matter continues to form collapsed structures, whereas the baryons are held out of these structures by the pressure support enforced by the minimum temperature.

In Figure 9 we calculate the baryon to dark matter number density ratio as a function of baryonic overdensity. The baryon to dark matter ratio is defined as  $n_{\text{bary}}/n_{\text{dm}} = \Omega_{\text{dm}}\rho_{\text{bary}}/\Omega_{\text{bary}}\rho_{\text{dm}}$ , so that  $n_{\text{bary}}/n_{\text{dm}} > 1$  corresponds to baryon enrichment, while  $n_{\text{bary}}/n_{\text{dm}} < 1$  implies baryon depletion. There is a clear trend for the highest density material to be baryon enriched, implying that the cores of the most collapsed structures are relatively enriched in baryons compared with the universal average. This trend persists even in the  $M_J > 0$  simulations, though it is not as pronounced as in the  $M_J = 0$  case. There is no evidence that a significant fraction of the baryons exist in regions which are dark matter enhanced. In all simulations underdense material appears to lie near the universal average mixture  $n_{\text{bary}}/n_{\text{dm}} \sim 1$ . We also note a trend with resolution, such that the higher the resolution of the simulation, the greater the baryon enrichment found in overdense regions.

A simple physical picture can account for these trends. So long as the density evolution is in the linear regime ( $\delta\rho/\rho \ll 1$ ), the dark matter and baryons evolve together, remaining at the universal mix of  $n_{\text{bary}}/n_{\text{dm}} \sim 1$ . During this linear phase the pressure support (barring any imposed minimum pressure) is orders of magnitude less important than the gravitational term, so the baryon/dark matter fluid evolves as a pressureless gas. Once nonlinear collapse begins ( $\delta\rho/\rho \gtrsim 1$ ), the baryons rapidly fall inward with the dark matter until they collide near the potential minimum. At this point the baryon gas shocks, converting the majority of its kinetic energy into thermal energy, and it stops, forming a hot pressure supported gas at the bottom of the potential well. In the case with a minimum pressure support, the collapse proceeds until the pressure term (due to the increase in density) builds sufficiently to impede the baryons infall, at which point the baryons slow, separate from the infall, and shock. In either case the dark matter forms a more diffuse structure supported by velocity dispersion. This process leads to the generic patterns noted above: on scales below which the collapse has become nonlinear, the baryons tend to be characteristically more clustered than the dark matter, at least down to the minimal point set by the Jeans scale. In either case the critical factor determining exactly when the baryons separate from the general inflow is the point at which shocking sets in. We also know from the numerical observations that this process is resolution dependent, and in fact the baryon enrichments we see for the  $M_J = 0$  case in Figure 9 must represent lower limits to the “true” baryon enrichment. The enrichments noted for the  $M_J > 0$  simulations should be reliable, to the extent that the specific minimum temperature chosen is reasonable.

It is somewhat puzzling to note that our measured positive biasing of the baryons in collapsed structures is at odds with previously published results. In a study of the cluster formation under the standard  $\Omega = 1$  Cold Dark Matter (CDM) model, Evrard (1990) finds that while outside of the cluster environment the baryons and dark matter simply track the universal average mix, the baryon fraction within the cluster is in fact somewhat lowered.

Kang et al. 1994 examine a larger volume of an  $\Omega = 1$  CDM cosmology, and find that not only are the overdense regions baryon depleted, but that their underdense, void structures are baryon enriched. There are several possible explanations for this disagreement. One possibility is that this represents a geometric effect, in that our experiments are 2-D, while these other studies employ fully 3-D simulations. In our simulations, the “filaments” actually represent walls, and the most collapsed knots are best interpreted as cross-sections through tubular filaments. The processes of collapsing to a plane, a line, or a point are certainly different processes, and the isotropy of pressure support makes these structures progressively more difficult to form. In a 1-D planar collapse, for instance, it is well known that the central collapse plane will be baryon enriched, while the question of whether or not a cluster is baryon enriched or depleted is still hotly debated. We see some evidence for this effect in Figure 9. Looking particularly at the upper dashed lines in this figure (representing the baryon enrichment at which 90% of the mass at that overdensity lies below) we note our most extreme enrichments occur at moderate overdensities, roughly in the range  $\rho_{\text{bary}}/\bar{\rho}_{\text{bary}} \sim 10^1 - 10^2$ . This extremely baryon enriched material represents the “filaments” in our simulations (walls in 3-D). It is also possible that resolution effects play a role here. As pointed out previously, we find a strong resolution dependence, such that finite resolution tends to underestimate the fraction of high density, collapsed baryonic material. Evrard (1990) uses  $16^3$  SPH nodes to represent his baryon component, which for the scale of his box is equivalent to our lowest resolution simulations. Kang et al. (1994) use an entirely different technique to simulate the hydrodynamics, which relies upon a fixed grid to represent the baryons. This limits their spatial resolution so that typical clusters are only a handful of cells across. It is also important to compare these quantities in the same manner. In Figure 9 we calculate the baryon to dark matter mixture in a manner which follows the baryon mass, since we sample at the positions of the baryon particles. This naturally gives the greatest weight to the most prominent baryonic structures. Kang et al. (1994) calculate this distribution in a manner which is volume weighted, which will tend to give the greatest weight to underdense, void like regions. Since the baryon fraction appears to be a function of environment, these differences can be significant. Without further study, it is difficult to know the true reason for this discrepancy, or how the actual baryon/dark matter ratio should evolve.

## 5. Discussion

The results of this investigation can be broken into two broad categories: what is revealed about the physics of hierarchical collapse in a mixed baryonic/dark matter fluid, and what is learned about the numerics of simulations of this process. We find that the dark

matter converges to a consistent state on resolved scales, so long as the nonlinear collapse scales are well resolved. Increasing the resolution of the experiment does not fundamentally alter the dark matter distribution, but simply yields more detailed information about the small scale collapsed structures. This is in agreement with previous, purely collisionless studies, though we demonstrate this here including a collisional component.

The numerical story is quite different for the collisional baryonic gas. We find that in the case where we do not impose a fundamental physical resolution scale in the baryons, the simulation results do not converge with increasing resolution. Rather, as the numerical resolution of the experiment is increased, the collapsed fraction of the baryons is systematically altered toward a higher density, more tightly bound, and less strongly shocked state. The physical reason for this behaviour is the presence of shocks, which allows the evolution on small scales to affect the overall state of the baryonic mass. With improving resolution the simulation is able to resolve the collapse of smaller structures at earlier times. The smaller scale (and therefore earlier) the resolved collapse, the weaker the resulting shock is found to be. This effect is most obvious in Figure 8, where there is a systematic trend of higher density/more weakly shocked material with increasing resolution.

The fact that the dark matter converges in general with resolution, while the baryons do not, highlights a fundamental difference in the physics of these two species. While both dark matter and baryon fluids react to the global and local gravitational potential, the baryons are additionally subject to purely local hydrodynamical phenomena – most prominently shocking in this case. Once strong shocking sets in these hydrodynamical effects can rise to rival the gravitational force on the baryonic fluid, allowing the baryons to be strongly influenced by interactions on small scales in ways which the dark matter is not. This implies that such small scale interactions can be just as important as the large scale forces in determining the final state of the baryons. In other words, for the dark matter there is no back reaction from small to large scales, whereas the baryons are strongly influenced by interactions on small scales. In the coupling of these physical processes, gravitation dominates the large scale structure, but hydrodynamics affects the local arrangements and characteristics of the baryonic gas. If we want the quantitative results of such studies to be reliable, we must have reason to believe that the localized hydrodynamical processes are adequately resolved.

This gloomy picture is alleviated by an important physical effect: the Jeans mass. Introducing a minimum temperature (and therefore pressure support) into the baryons creates a fundamental length/mass scale, below which the baryons are supported by pressure against any further collapse or structure formation. We find that once we introduce such a minimal scale into the baryonic component, the simulation results converge as this scale

is resolved. This convergence holds even though the dark matter component continues to form structures below the baryon Jeans scale. Although the Jeans scale is dependent upon the local density, we find that the global Jeans scale defined using the background density is adequate to define the critical resolution necessary for the hydrodynamics to converge. This therefore describes an additional resolution scale necessary for hydrodynamical simulations to meet, much as the nonlinear mass scale represents the crucial resolution necessary for purely gravitational systems. Furthermore, our experiments indicate that equation (4) is a reasonable estimate of an SPH simulation’s true mass resolution, since we find that the threshold  $M_R \lesssim M_J$  marks the point at which convergence is achieved.

In these experiments we have tested the effects of the Jeans mass in an idealized framework by simply imposing an arbitrary minimum temperature into our system, but there is reason to believe that such minimum temperatures should exist in the real universe. Based upon observations such as the Gunn-Peterson test (Gunn & Peterson 1965), it is known that the IGM is highly ionized out to redshifts  $z \lesssim 5$ , which implies a minimum temperature for the IGM of at least  $T \gtrsim 10^4$ . Assuming an Einstein-de Sitter cosmology, a minimum temperature of  $T \sim 10^4$  requires a minimum spatial resolution (via eq. [2])

$$\lambda_J \sim 0.777 (1+z)^{-3/2} \left( \frac{\mu}{0.6} \right)^{-1/2} \left( \frac{T}{10^4 \text{K}} \right)^{1/2} h^{-1} \text{Mpc}, \quad (6)$$

which equates to a baryon mass resolution of (eq. [3])

$$M_R \lesssim \Omega_{\text{bary}} M_J \sim 6.82 \times 10^{10} \Omega_{\text{bary}} (1+z)^{-3/2} \left( \frac{\mu}{0.6} \right)^{-3/2} \left( \frac{T}{10^4 \text{K}} \right)^{3/2} h^{-1} M_{\odot}. \quad (7)$$

This limit can also be expressed in terms of a minimum circular velocity, which has the advantage of being independent of redshift. The minimum circular velocity can be found as a function of the minimum temperature by relating the kinetic energy necessary for dynamical support to the internal energy for equivalent pressure support (Thoul & Weinberg 1996), yielding

$$v_{\text{circ}} = \left( \frac{2kT}{\mu m_p} \right)^{1/2} \sim 16.6 \left( \frac{\mu}{0.6} \right)^{-1/2} \left( \frac{T}{10^4 \text{K}} \right)^{1/2} \text{km/sec.} \quad (8)$$

In our  $M_J > 0$  simulations if we choose to call the scale at which RMS mass fluctuation is  $\Delta M/M \sim 0.5$  to be  $8 h^{-1} \text{Mpc}$  at the final expansion, then our box scale is  $L = 64 h^{-1} \text{Mpc}$  and the minimum temperature corresponds to  $T_{\text{min}} \sim 10^6 \text{K}$ . While there are some suggestions that the intergalactic medium could be heated to temperatures as hot as  $10^6 \text{K}$  (through mechanisms such as large scale shocks of the IGM), clearly these simulations do not meet our criteria if we wish to consider photoionization as setting the minimum temperature. It is also not clear that the current generation of large-scale hydrodynamical cosmological simulations meet this criterion, but it should be achievable.

It is still unclear whether or not in the case with no minimum temperature imposed the baryon distribution will eventually converge. It is well known that in a purely gravitational system, as structure builds and smaller dark matter groups merge into larger structures, the dark matter “forgets” about the earlier small scale collapses as such small structures are incorporated into larger halos and disrupted. This is why the dark matter results converge once the nonlinear mass scale is resolved. While it is evident from studies such as this that the baryons maintain a longer memory of their previous encounters, it seems likely that as the baryon gas is progressively processed through larger scale and stronger shocks, at some point the previous evolution should become unimportant. At exactly what level this transition is reached remains uncertain, however, as we see no evidence for such convergence here.

Radiative cooling must be accounted for in order to model processes such as galaxy formation, and the inclusion of radiative cooling can only exacerbate the non-convergence problems we find here. The amount of energy per unit mass dissipated by radiative cooling is proportional to the density, and we have already noted that the trend with finite resolution is to underestimate the local gas density and overestimate the temperature. Given these tendencies, it is not difficult to envision problems for finite resolution simulations which will tend to underestimate the effectiveness of radiative cooling in lowering the temperature (and therefore pressure support) of the shocked gas. This could lead to perhaps drastic underestimates of the fraction of cold, collapsed baryons for a given system, and therefore strongly influence the inferred galaxy formation. Evrard et al. (1994) note this effect when comparing their high and low resolution 3-D simulations. They find that altering their linear resolution by a factor of two (and therefore the mass resolution by a factor of eight) changes the measured total amount of cold collapsed baryons by a factor of  $\sim 3$ . They attribute this change to just the sort of problems we discuss here. Weinberg, Hernquist, & Katz (1996) report similar findings and interpretation for simulations with a photoionizing background. It therefore seems likely it is all the more important to resolve the minimum mass scale set by the minimum temperature in systems with radiative cooling.

We find that the majority of the baryonic mass undergoes strong shocking so long as the nonlinear mass scale exceeds the Jeans mass. At infinite resolution in the  $M_J = 0$  case, it is possible that all of the baryonic material undergoes shocking. As anticipated from previous investigations, the highest density collapsed fraction is characteristically less shocked as compared with later infalling material from larger regions. The underlying cause for this behavior is the fact that potential wells deepen as structure grows. The highest density material is that which collapses earliest due to the smallest scale perturbations. This material falls into relatively shallow potential wells, and is only weakly shocked. As the structures continue to grow, progressively larger scales go nonlinear and collapse.

The potential wells deepen and infalling material gains more energy, resulting in stronger shocking and higher temperatures.

Hydrodynamics can also play an important role in determining the distribution of the baryon mass, particularly in collapsed structures. In the absence of external mechanisms to heat the baryons (such as energy input from photoionization), during the linear phase of structure growth the baryons evolve as a pressureless fluid and simply follow the dominant dark matter. Once nonlinear collapse sets in, the baryons fall to the potential minimum, shock, convert their kinetic energy to thermal energy, and settle. In contrast, the dark matter simply passes through the potential minimum and creates a more diffuse structure supported by the anisotropic pressure of random velocities. This difference gives rise to a characteristic pattern in the baryon/dark matter ratio. Wherever the evolution is still linear, the baryons and dark matter simply remain at the universal mix. With the onset of nonlinear collapse, the baryons fall to the minimum of the potential well where they form a baryon enriched core, surrounded by a dark matter rich halo. We find that even in the absence of radiative cooling the cores of collapsed structures can become baryon enriched by factors of  $n_{\text{bary}}/n_{\text{dm}} \sim 2$  or more, though this value is likely resolution and dimension dependent. If the thermal energy of the baryons is raised to the point that it rivals the potential energy during the collapse, the baryons will become pressure supported and stop collapsing at that point. In all cases we find that the dark matter is relatively unaffected by the baryon distribution. This is due to the fact that the dark matter dominates the mass density, and therefore the gravitational potential. In general it appears that under a dark matter dominated scenario hydrodynamics can substantially alter the characteristics of the baryonic material (and therefore the visible universe), such that it does not directly follow the true mass distribution which is dominated by the the dark matter.

We would like to thank David Weinberg for inspiring this project, and for many useful discussions during its course as well. We would also like to thank the members of Ohio State’s Astronomy Department for the use of their workstations both for performance and analysis of many of the simulations. JMO acknowledges support from NASA grant NAG5-2882 during this project. Some of these simulations were performed on the Cray Y/MP at the Ohio Supercomputer Center.

## 6. References

Anninos, P., & Norman, M. L. 1996, ApJ, 459, 12

Binney, J. & Tremaine, S. 1987, *Galactic Dynamics*, (Princeton: Princeton University Press)

Beacom, J. F., Dominik, K. G., Melott, A. L., Perkins, S. P., & Shandarin, S. F. 1991, ApJ, 372, 351

Cen, R., & Ostriker, J. 1992a, ApJ, 393, 22

Cen, R., & Ostriker, J. 1992b, ApJ, 399, L113

Evrard, A. E. 1990, ApJ, 363, 349

Evrard, A. E., Summers, F. J., & Davis, M. 1994, ApJ, 422, 11

Gunn, J. E., & Peterson, B. A. 1965, ApJ, 142, 1633

Kang, H., Cen, R., Ostriker, J. P., & Ryu, D. 1994, ApJ, 428, 1

Katz, N., Hernquist, L., & Weinberg, D. H. 1992, ApJ, 399, L109

Little, B., Weinberg, D. H., & Park, C. 1991, MNRAS, 253, 295

Melott, A. L., & Shandarin, S. F. 1990, Nature, 346, 633

Navarro, J. F., & White, S. D. M. 1994, MNRAS, 267, 401

Owen, J. M, Villumsen, J. V., Shapiro, P. R., & Martel, H. 1996, submitted ApJS December 1995

Shapiro, P. R., Giroux, M. L, & Babul, A. 1994, ApJ, 427, 25

Shapiro, P. R., & Struck-Marcell, C. 1985, ApJS, 57, 205

Steinmetz, M., & Müller, E. 1994, A&A, 281, L97

Thoul, A. A., & Weinberg, D. H. 1996, preprint

Weinberg, D. H., Hernquist, L., & Katz, N. 1996, submitted to ApJ, astro-ph/9604175

White, S. D. M., & Rees, M. J. 1978, MNRAS, 183, 341

Fig. 1.— The ratio of the Jeans mass to the resolved mass ( $M_J/M_R$ ) as a function of expansion for each of the three resolutions used in this paper ( $N = 64^2, 128^2, 256^2$ ) for the  $M_J > 0$  case. The Jeans mass is calculated using the average background density of the universe at each expansion.

Fig. 2.— Dark matter overdensities ( $\rho_{\text{dm}}/\bar{\rho}_{\text{dm}}$ ) for  $M_J = 0$  simulations. Panels arranged with increasing resolution along rows ( $N = 64^2, 128^2, 256^2$ ), and increasing cutoff in initial input perturbation spectrum down columns ( $k_c = 32, 64, 128$ ). Part a) shows results using the full resolution of each simulation, while b) is calculated after resampling the simulations down to equivalent  $N = 64^2$  resolution. All simulations are shown at the final time slice (expansion factor  $a/a_i = 60$ ), with grey scale intensity scaled logarithmically with dark matter density.

Fig. 3.— Normalized dark matter overdensity distribution functions  $f(\rho_{\text{dm}}/\bar{\rho}_{\text{dm}})$  for  $M_J = 0$  (solid lines) and  $M_J > 0$  (dotted lines) simulations. Part a) shows results for full simulations, while part b) shows all simulations degraded to equivalent  $N = 64^2$  resolution.

Fig. 4.— Baryon overdensities  $\rho_{\text{bary}}/\bar{\rho}_{\text{bary}}$  for a)  $M_J = 0$  at  $a/a_i = 30$ , b)  $M_J = 0$  at  $a/a_i = 60$ , c)  $M_J > 0$  at  $a/a_i = 30$ , and d)  $M_J > 0$  at  $a/a_i = 60$ . Panels arranged as in Figure 2.

Fig. 5.— Baryon overdensities for  $k_c = 32$  simulations, resampled to  $N = 64^2$  resolution as in Figure 2b. Note these panels represent the same simulations as the top rows of the previous figures. Shown are expansion factors a)  $a/a_i = 30$  and b)  $a/a_i = 60$ . Panels are arranged with increasing simulation resolution ( $N = 64^2, 128^2, 256^2$ ) along rows, and increasing baryon Jeans mass ( $M_J = 0, M_J > 0$ ) down columns.

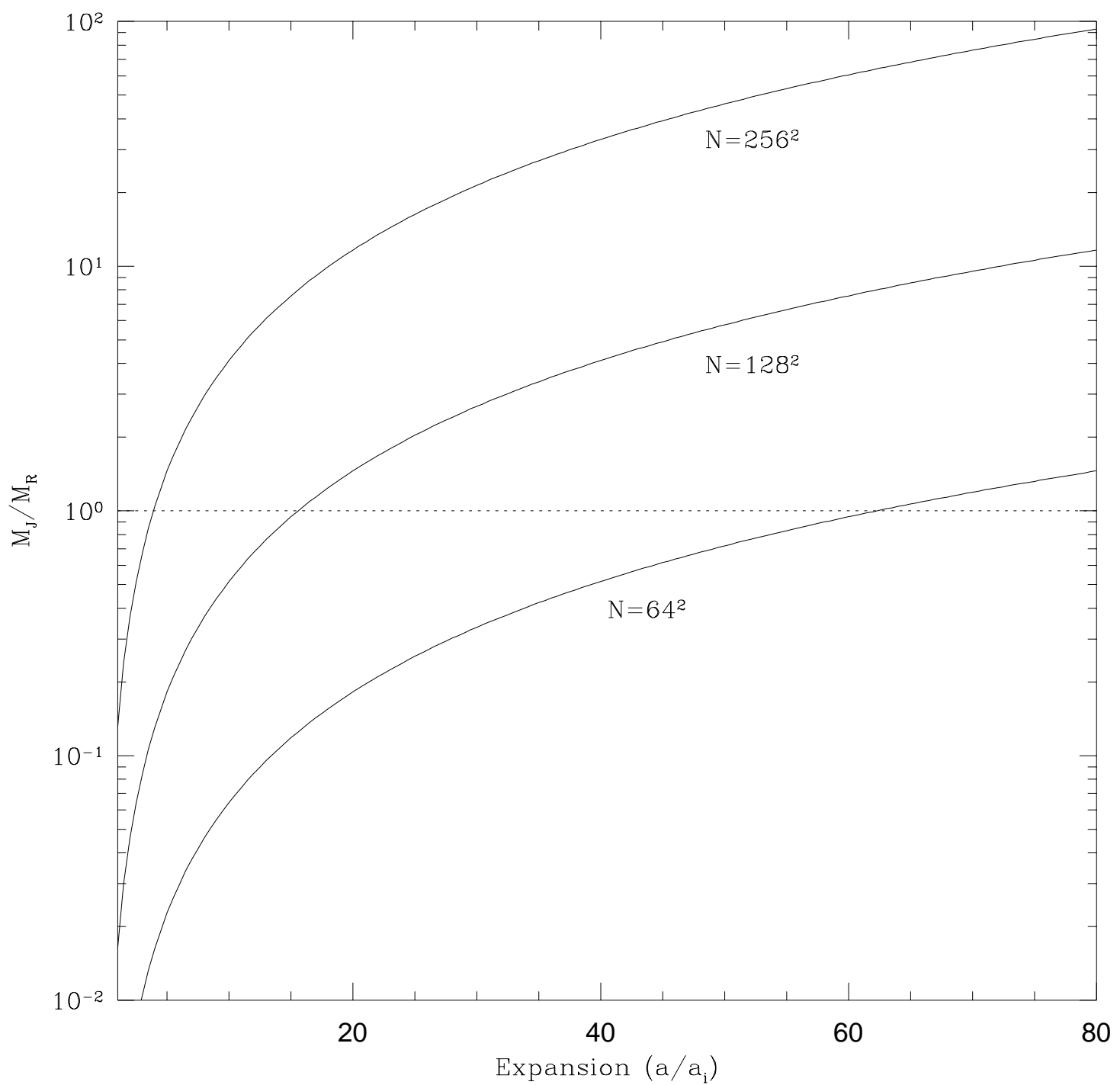
Fig. 6.— Normalized baryon overdensity distribution functions  $f(\rho_{\text{bary}}/\bar{\rho}_{\text{bary}})$  for  $M_J = 0$  (solid lines) and  $M_J > 0$  (dotted lines). We show the full resolution results for a)  $a/a_i = 30$  and b)  $a/a_i = 60$ , as well as results when each simulation is degraded to  $N = 64^2$  resolution at c)  $a/a_i = 30$  and d)  $a/a_i = 60$ . Panels arranged as in Figure 3.

Fig. 7.— Kolmogorov-Smirnov statistic  $D$  comparing  $f(\rho_{\text{bary}})$  between simulations. Each line type corresponds to one simulation which is compared to each simulation listed on the ordinate axis, where the simulations are denoted as  $N : k_c$ . Note that the K-S statistic for comparing an individual simulation to itself is formally  $D = 0$ , but for the sake of clarity we have interpolated over these points in this plot. The panels are arranged with Jeans mass  $M_J$  increasing along rows, and expansion  $a/a_i$  increasing down columns.

Fig. 8.— Baryon mass distribution for the  $M_J = 0$  simulations as a function of overdensity

and temperature  $f(\rho_{\text{bary}}/\bar{\rho}_{\text{bary}}, T)$  (upper row) and  $f(\rho_{\text{bary}}/\bar{\rho}_{\text{bary}}, T/T_{ad})$  (lower row).  $T_{ad} = T_0(\rho/\rho_0)^{\gamma-1}$  is defined as the temperature the gas would have due solely to adiabatic processes. Panels arranged as in Figure 6.

Fig. 9.— Average baryon to dark matter mixture as a function of baryon overdensity at  $a/a_i = 60$ . The baryon to dark matter mixture is defined as  $n_{\text{bary}}/n_{\text{dm}} = \Omega_{\text{dm}}\rho_{\text{bary}}/\Omega_{\text{bary}}\rho_{\text{dm}}$ , so that  $n_{\text{bary}}/n_{\text{dm}} > 1$  represents baryon enriched material, while  $n_{\text{bary}}/n_{\text{dm}} < 1$  is baryon depleted. In each panel the solid line shows the measured average baryon to dark matter mixture, while the dashed lines represent the mixtures such that 10% of the mass at each overdensity is above and below the enclosed region. The dotted line shows the universal average  $n_{\text{bary}}/n_{\text{dm}} = 1$ . The top and bottom rows represent the  $M_J = 0$  and  $M_J > 0$  simulations, respectively.

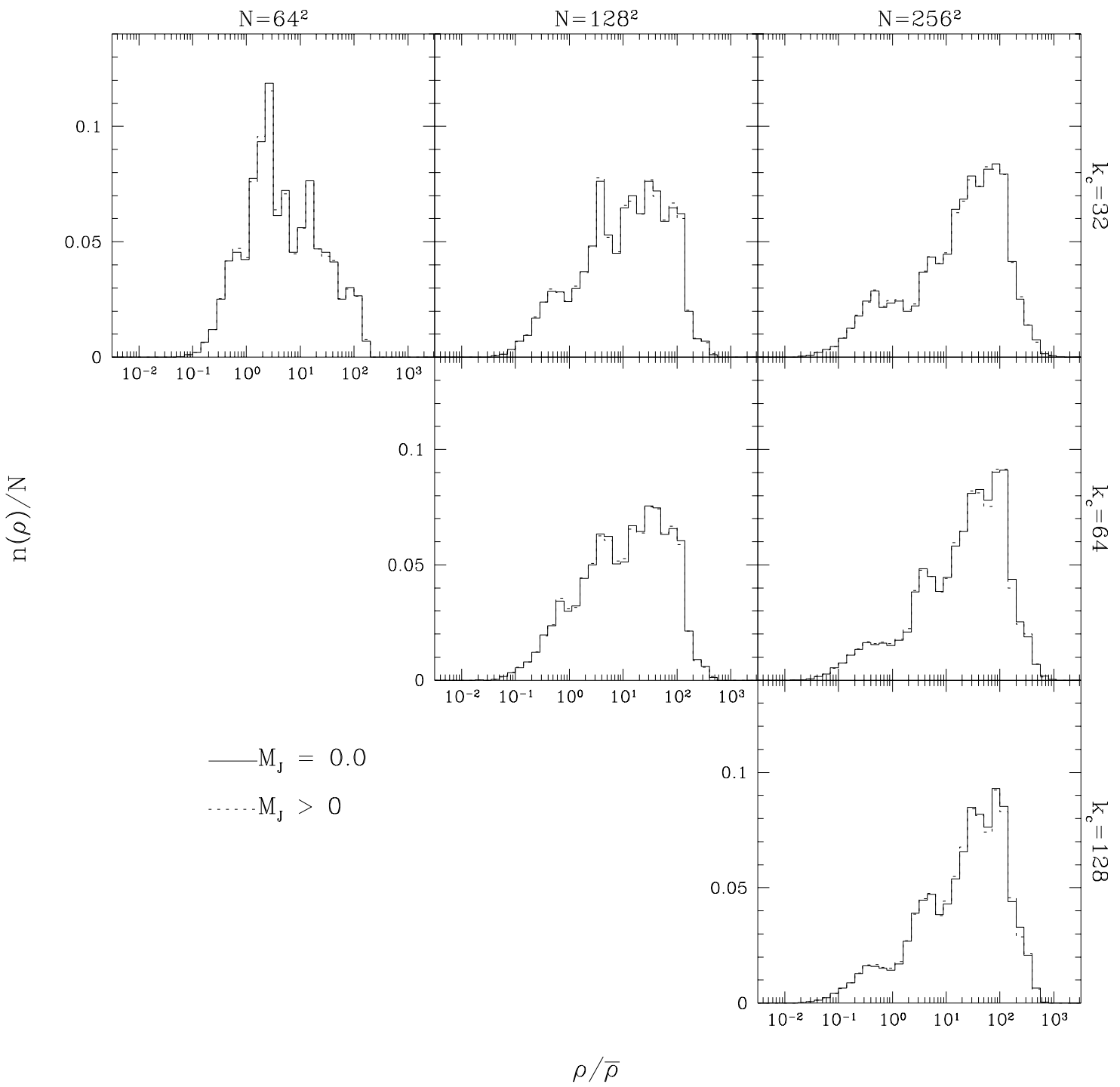


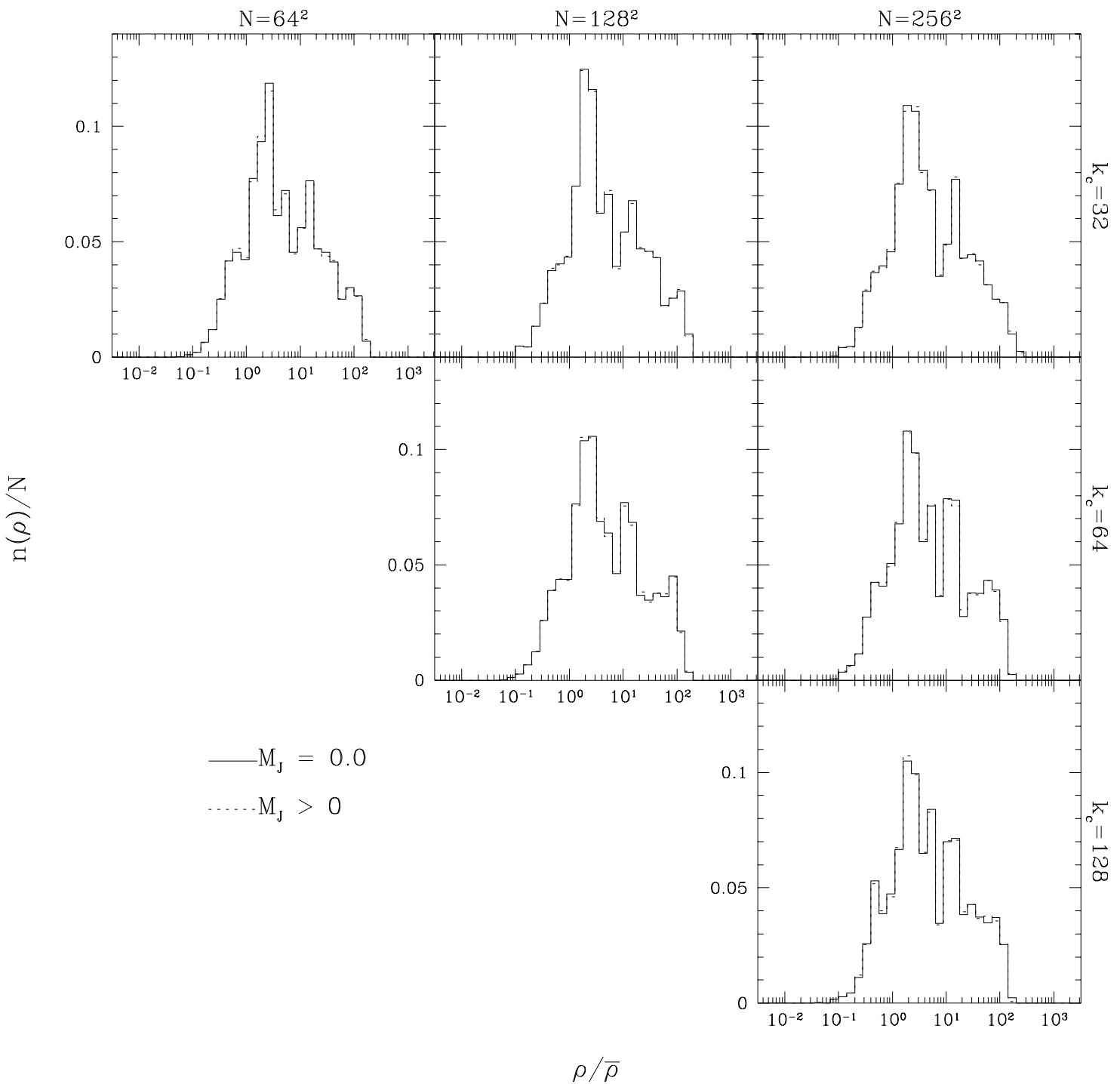
This figure "Fig02a\_bw.jpg" is available in "jpg" format from:

<http://arxiv.org/ps/astro-ph/9603156v3>

This figure "Fig02b\_bw.jpg" is available in "jpg" format from:

<http://arxiv.org/ps/astro-ph/9603156v3>





This figure "Fig04a\_bw.jpg" is available in "jpg" format from:

<http://arxiv.org/ps/astro-ph/9603156v3>

This figure "Fig04b\_bw.jpg" is available in "jpg" format from:

<http://arxiv.org/ps/astro-ph/9603156v3>

This figure "Fig04c\_bw.jpg" is available in "jpg" format from:

<http://arxiv.org/ps/astro-ph/9603156v3>

This figure "Fig04d\_bw.jpg" is available in "jpg" format from:

<http://arxiv.org/ps/astro-ph/9603156v3>

This figure "Fig05a\_bw.jpg" is available in "jpg" format from:

<http://arxiv.org/ps/astro-ph/9603156v3>

This figure "Fig05b\_bw.jpg" is available in "jpg" format from:

<http://arxiv.org/ps/astro-ph/9603156v3>

